Published in final edited form as:
Biochem Pharmacol. 2008 June 1; 75(11): 2147–2156. doi:10.1016/j.bcp.2008.02.027.

Sarcoplasmic reticulum Ca^{2+} release channel ryanodine receptor (RyR_2) plays a crucial role in aconitine-induced arrhythmias

Min Fu[a,b], **Ru-Xin Li**[a], **Li Fan**[c], **Guo-Wei He**[c], **Kent L. Thornburg**[d,**], and **Zhao Wang**[a,*]

[a]School of Medicine and Department of Biological Sciences and Biotechnology, Tsinghua University, Beijing 100084, People's Republic of China

[b]Beijing University of Chinese Medicine, Beijing 100029, People's Republic of China

[c]Cardiovascular Research, Starr Academic Center for Cardiac Surgery, Heart & Vascular Institute, Providence St. Vincent Medical Center, Portland, OR 97225, USA

[d]Heart Research Center, L464, Oregon Health & Science University, Portland, OR 97239, USA

Abstract

The present study established a model of RyR_2 knockdown cardiomyocytes and elucidated the role of RyR_2 in aconitine-induced arrhythmia. Cardiomyocytes were obtained from hearts of neonatal Sprague–Dawlay rats. siRNAs were used to down-regulate RyR_2 expression. Reduction of RyR_2 expression was documented by RT-PCR, western blot, and immunofluorescence. Ca^{2+} signals were investigated by measuring the relative intracellular Ca^{2+} concentration, spontaneous Ca^{2+} oscillations, caffeine-induced Ca^{2+} release, and L-type Ca^{2+} currents. In normal cardiomyocytes, steady and periodic spontaneous Ca^{2+} oscillations were observed, and the baseline $[Ca^{2+}]_i$ remained at the low level. Exposure to 3 μM aconitine increased the frequency and decreased the amplitude of Ca^{2+} oscillations; the baseline $[Ca^{2+}]_i$ and the level of caffeine-induced Ca^{2+} release were increased but the L-type Ca^{2+} currents were inhibited after application of 3 μM aconitine for 5 min. In RyR_2 knockdown cardiomyocytes, the steady and periodic spontaneous Ca^{2+} oscillations almost disappeared, but were re-induced by aconitine without affecting the baseline $[Ca^{2+}]_i$ level; the level of caffeine-induced Ca^{2+} release was increased but L-type Ca^{2+} currents were inhibited. Alterations of RyR_2 are important consequences of aconitine-stimulation and activation of RyR_2 appear to have a direct relationship with aconitine-induced arrhythmias. The present study demonstrates a potential method for preventing aconitine-induced arrhythmias by inhibiting Ca^{2+} leakage through the sarcoplasmic reticulum RyR_2 channel.

Keywords

RyR_2; Knockdown; Aconitine; Arrhythmia; Excitation–contraction coupling

*Corresponding author. Tel.: +86 10 6277 2240; fax: +86 10 6277 2675. zwang@tsinghua.edu.cn (Z. Wang). **Corresponding author. Tel.: +1 503 494 2305; fax: +1 503 494 8550. thornbur@ohsu.edu (K.L. Thornburg).

1. Introduction

Aconite tuber, roots of aconite (*Aconitum carmichaeli* or *A. kusnezofii*), is an important oriental herbal medicine used for centuries in China and other countries to therapeutically increase the peripheral temperature, relieve rheumatic pain and treat neurological disorders [1]. The pharmacological effects of Aconitum alkaloids include positive inotropic effects, analgesic, anti-inflammatory, and antirheumatic activity as well as neurotransmission actions [2–4]. Aconitine and its structurally related analogs are known to injure both the central nervous system and the heart [5]. Its cardiotoxicity consists primarily of arrhythmic effects and it has been used as an experimental tool to induce tachyarrhythmias in animal models [6]. In spite of its potential toxic effects, aconitine remains a popular home remedy for several ailments in China. Although most mechanisms postulated for aconitine toxicity focus on voltage-dependent Na^+ channels, little is known about its interaction with intracellular Ca^{2+} signals and Ca^{2+} handling proteins that regulate the cardiac excitation–contraction coupling (e–c coupling) system. We have shown previously that aconitine impairs the contractile function by disrupting the intracellular Ca^{2+} homeostasis in the cardiac e–c coupling of cultured cardiomyocytes and stimulating up-regulation of the type 2-ryanodine receptor (RyR_2) level significantly [7]. The present study was therefore designed to establish a model of RyR_2 knockdown (KD) cardiomyocytes and elucidate the role of RyR_2 in aconitine-induced arrhythmia.

In cardiac muscle, the intracellular Ca^{2+} stores and the sarcoplasmic reticulum (SR) Ca^{2+} release play prominent roles in cardiac contractile activation and relaxation [8–10]. Ca^{2+} release from SR through the cardiac RyR_2 channel is a fundamental event in cardiac muscle contraction, which is triggered by calcium-induced calcium release (CICR) [11]. Alterations in the sensitivity of RyR_2 to Ca^{2+} release activation have been implicated in diseases including malignant hyperthermia and heart failure [12–14]. Mutations in RyR_2 that are suspected to cause defective Ca^{2+} channel function and aberrant intracellular Ca^{2+} signals have recently been identified in catecholaminergic polymorphic ventricular tachycardia (CPVT) and arrhythmogenic right ventricular dysplasia (ARVD) patients [15]. Cardiomyocytes in RyR_2 gene knock-out (KO) mice show a decrease in the rate of spontaneous diastolic depolarization and an absence of calcium sparks [16].

We report here that RyR_2 gene expression was strongly reduced in cultured neonatal rat cardiomyocytes by exogenous transcription of small interfering RNAs (siRNAs). Moreover, we examined the effects of aconitine on the relative intracellular Ca^{2+} concentration, spontaneous Ca^{2+} oscillations, caffeine-induced Ca^{2+} release and L-type Ca^{2+} channel currents in control and RyR_2 KD cardiomyocytes.

2. Materials and methods

2.1. Animals and chemicals

Cardiomyocytes were obtained by dissociating hearts of neonatal Sprague–Dawlay rats (1–3 days old). The experimental protocol for animals was approved by the Medical Ethical Committee of Tsinghua University. Aconitine (content ≥98%) was purchased from the National Institute for the Control of Pharmaceutical & Biological Products (China).

2.2. RyR_2 gene knockdown techniques

2.2.1. Preparation of siRNAs for targeting on RyR_2 gene—siRNAs were designed by Ambion (Ambion Inc., USA) according to the guidelines for effective knockdown. Three double-stranded siRNAs for targeting rat RyR_2 gene were as follows: target 1 for RyR_2 (siRNA1), 5′-CCUUGAACAGAAAUCUAAGtt-3′ (sense) and 5′-CUUAGAUUUCUGUUCAAGGtg-3′ (antisense); target 2 for RyR_2 (siRNA2), 5′-CCCUCAGAGAUCAAAGAAAtt-3′ (sense) and 5′-UUUCUUUGAUCUCUGAGGGtg-3′ (antisense); target 3 for RyR_2 (siRNA3), 5′-GCCAUGAAAAGAGUUGAUCtt-3′ (sense) and 5′-GAUCAACUCUUUUCAUGGCtt-3′ (antisense). The positive control siRNAs (anti-GAPDH siRNA) were purchased from Ambion. All siRNAs were provided in a freeze-dried, preannealed, HPLC-purified form (>80%). 20 nmol of annealed siRNA was resuspended into 200 μl RNA-free ddH_2O as a stock solution at the concentration of 100 μM, and stored at −70 °C until required.

2.2.2. Cell cultures and siRNA transfection—Primary cardiomyocyte cultures were obtained as previously described [17]. Cells were seeded into six-well plates at a final density of $1.5–3 \times 10^5$ cells per well in DMEM/F12 media (Invitrogen Corporation, USA) supplemented with 10% fetal bovine serum (FBS) (Hyclone Laboratories Inc., USA) for 3 days under normal growth conditions (37 °C, 91% humidity and 5% CO_2). All siRNAs were transfected into cardiomyocytes monolayers by using the siPORT™ NeoFX™ lipid-based reagent for reverse transfection (Ambion Inc., USA) according to the transfection protocol. After 6 h of transfection, the complexes were removed from the six-well plates. 2 ml fresh media containing 10% FBS was added to the plates. After 6 and 72 h, cardiomyocytes were used for subsequent experiments, each of which was performed at least three times. The controls were analyzed in parallel.

To optimize the contribution of the siRNA amount and the siPORT™ NeoFX™ volume to transfection efficiency in six-well plates, total volume of siRNA (2 μM) was varied between 1.25 and 37.5 μl, and siPORT™ NeoFX™ volume was varied between 2 and 6 μl per well. The cytotoxicity was evaluated by MTT assays. Down-regulation of RyR_2 expression was identified by RT-PCR, western blot, and immunofluorescence analyses.

2.2.3. RT-PCR analyses—Total cellular RNA was extracted by PUREGENE™ RNA isolation kit (Gentra Systems, USA). Spectrophotometry at 260 and 280 nm was performed to measure the amount and purity of RNA. The specific primers used for RT-PCR are described in Ref. [7]. The GADPH primer was as follows: sense, 5′-TTGGCCGTATTGGCCGC-3′; antisence, 5′-GTGCCATTGAAC-TTGCCGTG-3′. The PCR condition was 95 °C for 1 min 30 s, 94 °C for 30 s, 52–60 °C for 40 s, and 72 °C for 30 s, 35 cycles, with a final extension for 5–7 min at 72 °C. In all experiments, the threshold count values were normalized to the internal control of GAPDH before calculating the changes for all of the genes. The products were separated by 1.5% agarose gel stained with ethidium bromide (EB). Intensity of the DNA bands was analyzed using the Totallab TL100 software (Nonlinear Inc., USA).

2.2.4. Western blot analyses—Protocols described in reference 18 were followed [18]. Protein samples (120 μg of total protein per lane) were separated by 5% SDS-PAGE gels for RyR and transferred to PVDF membranes. The membranes were probed with the monoclonal anti-RyR (1:2500, MA3-925) (Affinity Bioreagents, USA). A peroxidase-conjugated goat anti-mouse IgG was used as a secondary antibody (1:5000) (Affinity Bioreagents, USA). β-Actin was used as the internal standard for analysis of the protein. Signals were detected using the super signal ECL substrate (Pierce Biotechnology Inc., USA). The Totallab TL100 software was used to analyze the protein bands (Nonlinear Inc., USA).

2.2.5. Immunofluorescence assays—For immunofluorescence assays, cardiomyocytes were fixed with the mixture of methanol and acetone (v/v, 1:1) and blocked in 10% horse serum for 30 min at 37 °C. They were then incubated with the primary monoclonal anti-RyR (1:1000, MA3-925) (Affinity Bioreagents, USA) for 1 h at 37 °C, followed by goat anti-mouse IgG–FITC (1:100) secondary antibody (Santa Cruz Biotechnology Inc., USA) in dark chamber for 30 min at 37 °C. After that, cells were subsequently stained with PI (5 μg/ml, PBS) for 5 min and detected using a ZEISS LSM510 META laser-scanning confocal microscope (MIC Bergen, USA). Fluorescence recordings were done with either 488 nm laser excitation (520LP emission) or 543 nm laser excitation (580LP emission).

2.3. Assays of Ca^{2+} signals

2.3.1. Assays of the spontaneous Ca^{2+} oscillations and the relative intracellular Ca^{2+} concentration by Ca^{2+} imaging—Ca^{2+} imaging experiments were performed to measure the spontaneous Ca^{2+} oscillations and the relative intracellular Ca^{2+} concentration in control and RyR_2 KD cardiomyocytes with aconitine-stimulation [19]. Cardiomyocytes were inoculated in 35 mm dishes (MatTeK Corporation, USA) and loaded with 5 μM fluo-3 AM (Sigma Chemical Co., USA). Intracellular fluo-3 AM was excited by a DG-4 quartz lamp filtered at 488 nm, and emission wavelengths were monitored with a 520 nm long-pass filter in 37 °C perfusion solution (in mM: 145 NaCl, 5.4 KCl, 0.5 $MgCl_2$, 1.2 $CaCl_2$, 5 HEPES, 5.5 Glucose, 0.3 NaH_2PO_4, pH 7.4) [20]. Rapid scanning of the observation field (5 s/scan) was used to minimize photo-oxidation artifacts. The images were recorded by a CoolSNAP fx CCD camera (Roper Scientific, USA). Ca^{2+} oscillations were recorded and analyzed using MetaFluor software (Universal Imaging Corporation, USA).

2.3.2. Assessments content of SR Ca^{2+} release stimulated by caffeine—To evaluate the SR Ca^{2+} loading state, caffeine (20 mM) was applied to stimulate Ca^{2+} release from SR. After the relative intracellular free Ca^{2+} concentration ($[Ca^{2+}]_i$) transients of the fluo-3 AM loaded cardiomyocytes became stable, a rapid pulse of 20 mM caffeine (200 ms) was applied to the cardiomyocytes via a micropipette (~4 μm at tip). The micropipette was placed downstream with respect to the superfusate flow, which prevented caffeine leaking out of the pipette from diffusing to the cardiomyocytes. Baseline values for $[Ca^{2+}]_i$ were measured in individual cells. Resting and peak $[Ca^{2+}]_i$ during caffeine application were each converted to total cytosolic Ca^{2+} taking into account estimated Ca^{2+} binding at high and low affinity sites. The difference ($\Delta[Ca^{2+}]_i$) was taken as the total level of caffeine-induced Ca^{2+}

release. Cells without treatment were initiated by a puff of caffeine to induce SR Ca^{2+} release. After washed out the caffeine with perfusion solution, cells were treated with 3 μM aconitine for 5 min, and then initiated with the puff of caffeine to induce SR Ca^{2+} release.

2.3.3. L-type Ca^{2+} currents assay by patch clamp—Intracellular Ca^{2+} currents were recorded using the whole-cell patch clamp technique. The culture media was replaced with the external solution (in mM: 120 NaCl, 5 KCl, 1 $MgCl_2$, 3.6 $CaCl_2$, 10 HEPES, 20 TEA, 0.001 TTX, pH 7.4 (TEAOH)) before recording. The patch pipettes (4–6 M resistance) were filled with the internal solution (in mM: 120 CsCl, 3 $MgCl_2$, 5 HEPES, 10 EGTA, 5 MgATP, pH 7.4 (CsOH)) [21]. Whole-cell path clamp recordings were made at room temperature (21–23 °C) with the Axopatch-200B amplifier (Axon Instruments, USA) in conjunction with pClamp9 software (Axon Instruments, USA). Cardiomyocytes were clamped at −40 mV and step depolarized to +50 mV in 10 mV increments. Ca^{2+} current recordings were filtered with a current filter at 5 kHz.

2.4. Statistical analyses

Data were presented as mean ± S.E. Differences between means were determined using the Student's *t*-test for paired observations. Differences were considered statistically significant when *p*-value <0.05.

3. Results

3.1. Maximal reduction of RyR_2 mRNA level was achieved by exogenous transcription of siRNA3 48 h after transfection

In order to examine the silencing specificity of the three siRNAs in primary cultured cardiomyocytes from hearts of neonatal SD rats (1–3 days), mRNA levels of RyR_2 were investigated by RT - PCR. Transfection of cardiomyocytes with the siRNA3 template led to significant reduction of mRNA level of RyR_2.

To further examine siRNA specificity, reduction of RyR_2 expression in cardiomyocytes after delivery of siRNA3 for 6–72 h was documented by mRNA level (semiquantitative RT-PCR) paralleled with the corresponding protein expression (western blot) (Fig. 1A and B). Changes in mRNA and protein levels of RyR_2 were noted in cardiomyocytes with siRNA transfection after 24 h. We can also see that changes in mRNA and protein levels after 48–72 h were more significant than other time point. But it was shown in MTT assays that cytotoxicity of the cardiomyocytes with transfection after 72 h was more obvious than that in cardiomyocytes with transfection after 48 h, so in the subsequent experiments, we use the KD cadiomyocytes with transfection after 48 h.

Of the three siRNAs, the maximal silencing effect of RyR_2 was achieved with the siRNA3 targeting rat RyR_2 gene from 2137 to 2155 bp. The silencing effects of siRNA1 and siRNA2 targeting 1850–1868 bp and 1902–1920 bp, respectively, were less obvious than that of siRNA3 (XM_341548). The optimal siRNA amount and siPORT™ NeoFX™ volume that yielded the best transfection efficiency in six-well plates were under the following conditions: total volume of media is 1 ml, total volume of siRNA (2 μM) is 5 μl, and the siPORT™ NeoFX™ volume is 4 μl per well.

3.2. The mRNA and protein levels of RyR_2 were increased by aconitine

To examine the effect of aconitine on RyR_2, RT-PCR, western blot, and immunofluorescence were used to examine RyR_2 expression. As illustrated in Fig. 2A and B, mRNA and protein levels were increased both in control and KD cardiomyocytes induced by 3 μM aconitine for 0.5 h. We can also see that alteration of RyR_2 expression in KD cardiomyocytes is more obvious rather than that in control cardiomyocytes. (mRNA level: from 100.05 ± 6.31 to 182.51 ± 17.85% in CN cardiomyocytes and from 22.76 ± 8.42 to 51.89 ± 12.33% in KD cardiomyocytes, respectively; protein level: from 100.08 ± 6.04 to 142.39 ± 9.61% in CN cardiomyocytes and from 35.12 ± 11.3 to 62.38 ± 6.74% in KD cardiomyocytes, respectively.)

Immunostaining was used to localize RyR_2 in cardiomyocytes (Fig. 2C). Fluorescence in cardiomyocytes stained with primary anti-RyR and FITC-labeled secondary antibodies was noted in control cardiomyocytes with cytosolic prominence likely caused by active RyR_2 expression. We observed the reduction of RyR_2 expression in all cardiomyocytes visible in the field, which indicates a very efficient siRNA delivery 48 h after transfection. We can also see in Fig. 2C that, consistent with RT-PCR and western blot results, RyR_2 fluorescence was significantly increased after exposure to 3 μM aconitine for 0.5 h in RyR_2 KD cardiomyocytes.

3.3. Aconitine-induced recovery of spontaneous Ca^{2+} oscillations without affecting the baseline $[Ca^{2+}]_i$ in RyR_2 KD cardiomyocytes

We used digital imaging technique to explore the effects of aconitine on spontaneous Ca^{2+} oscillations and the relative intracellular Ca^{2+} concentration (baseline $[Ca^{2+}]_i$) in control and RyR_2 KD cardiomyocytes (Fig. 3A and B). In control cardiomyocytes, steady and periodic spontaneous Ca^{2+} oscillations were observed, and the baseline $[Ca^{2+}]_i$ remained at low level. Application of 3 μM aconitine resulted in a significant increase in the frequency (nearly 2-fold higher, from 7.25 ± 0.25 to 13.75 ± 0.35, $p < 0.05$) and a decrease in the amplitude of spontaneous Ca^{2+} oscillations (from 159.41 ± 12.72 to 113.34 ± 3.34 $\Delta F/F_0$%, $p < 0.05$). A significant elevation of the baseline $[Ca^{2+}]_i$ (from 11.38 ± 1.07 to 82.14 ± 13.66 $\Delta F/F_0$%, $p < 0.01$) was also observed.

In contrast, in RyR_2 KD cardiomyocytes, steady and periodic spontaneous Ca^{2+} oscillations disappeared completely. Interestingly, application of 3 μM aconitine re-induced spontaneous Ca^{2+} oscillations (frequency: from 0.5 ± 0.29 to 4.4 ± 0.2, $p < 0.01$; amplitude: from 65.52 ± 6.66 to 73.45 ± 7.42 $\Delta F/F_0$%) without affecting the baseline $[Ca^{2+}]_i$ level (15.23 ± 3.38 vs. 17.93 ± 1.36 $\Delta F/F_0$%) (Fig. 3D–F).

3.4. The level of caffeine-induced Ca^{2+} release in the cardiomyocytes was increased by aconitine

The SR Ca^{2+} release from the SR was estimated by the traditional caffeine puff. The Ca^{2+} content released from SR during the caffeine contracture was measured as $\Delta F/F_0$%. Superimposed Ca^{2+} transients in control and RyR_2 KD cardiomyocytes were performed (Fig. 4A and B). It was shown that Ca^{2+} transients were relatively smaller in RyR_2 KD cardiomyocytes than those in control cardiomyocytes (164.25 ± 33.29 vs. 83.89 ± 28.36

$\Delta F/F_0$%). The alterations of transient amplitudes, however, were amplified significantly in both of these two kinds of cardiomyocytes when the caffeine contracture was done in 3 μM aconitine-containing perfusion solution for 5 min (CN cardiomyocytes: from 164.25 ± 33.29 to 254.17 ± 35.41 $\Delta F/F_0$%, $p < 0.05$; KD cardiomyocytes: from 83.89 ± 28.36 to 178.26 ± 29.32 $\Delta F/F_0$%, $p < 0.05$, respectively) (Fig. 4C).

3.5. L-type Ca^{2+} currents in cardiomyocytes were inhibited by aconitine

Current responses to a voltage step from −40 to 50 mV were recorded in control and RyR_2 KD cardiomyocytes and estimated as current density (A/F) (Fig. 5A and B). Both in control and KD cardiomyocytes, *I–V* curves showed that activation of L-type Ca^{2+} current began at −30 mV and peak currents occurred between 0 and +10 mV in the absence and presence of 3 μM aconitine (Fig. 5C and D).

Comparing the peak currents density at 10 mV, *I–V* relationships showed that L-type Ca^{2+} currents in RyR_2 KD cardiomyocytes were higher than those in control cardiomyocytes (52.84 ± 13.66 A/F vs. 75.77 ± 18.80 A/F). We can also see that both in control and RyR_2 KD cardiomyocytes, the L-type Ca^{2+} current density at peak current was significantly lower in the presence of 3 μM aconitine as compared to that in the absence of aconitine (Fig. 5C and D). L-type Ca^{2+} currents density in control cardiomyocytes was decreased by application of 3 μM aconitine (52.84 ± 13.66 A/F vs. 19.51 ± 4.01 A/F, $p < 0.05$). And that in RyR_2 KD cardiomyocytes was decreased from 75.77 ± 18.80 to 21.98 ± 2.44 A/F by application of 3 μM aconitine ($p < 0.05$) (Fig. 5E).

4. Discussion

The present study established a model of RyR_2 KD cardiomyocytes and found calcium homeostasis in these myocytes were seriously affected. In addition, we studied the possible role of RyR_2 in aconitine-induced arrhythmias by comparing the effects of the presence and absence of aconitine in control cardiomyocytes and in cardiomyocytes with reduced RyR_2 mRNA and protein levels. We concluded that alterations of RyR_2 are important consequences of aconitine-stimulation and activation of RyR_2 expression appear to have a direct relationship with aconitine-induced arrhythmias. This conclusion was mainly based on the observations that (1) aconitine induced up-regulation of RyR_2 mRNA and protein levels both in control and RyR_2 KD cardiomyocytes; (2) aconitine-induced recovery of spontaneous Ca^{2+} oscillations without affecting the baseline $[Ca^{2+}]_i$ in RyR_2 KD cardiomyocytes; (3) the level of caffeine-induced Ca^{2+} release in the cardiomyocytes was increased by aconitine; (4) L-type Ca^{2+} channel currents in cardiomyocytes were inhibited by aconitine. The present study therefore provides an insight into a useful method for preventing aconitine-induced arrhythmias by reducing Ca^{2+} leakage through the SR RyR_2 channel.

Mutations in the human RyR_2 gene have been shown to cause different forms of cardiac arrhythmias characterized by stress-, emotion-, and physical exercise-induced ventricular tachycardia (VT). However, the molecular and cellular mechanisms underlying these forms of ventricular arrhythmias are not clear [22]. It has been hypothesized that disease-associated RyR_2 mutations are likely to cause the channel to open spontaneously or to

increase its sensitivity to activation by luminal Ca^{2+} [23,24]. In an earlier study we found that aconitine could enhance mRNA and protein levels of RyR_2 gene [7]. We conjectured, on these grounds, that alterations in RyR_2 channel function induced by aconitine would influence the properties of SR Ca^{2+} release and spontaneous Ca^{2+} oscillations, and thus cause the occurrence of triggered arrhythmias. In order to elucidate the crucial role of RyR_2 in aconitine-induced arrhythmia, we use the RyR_2 gene KD cardiomyocytes model to further study the role of RyR_2 in aconitine-induced arrhythmic toxicity.

The siRNA method for reducing gene expression is a rapidly evolving tool in molecular biology. There are several methods for preparing siRNA [25]. Here, we report that reduction of RyR_2 gene expression can be obtained by the chemical synthesis siRNAs with the aid of lipid-based reagent for reverse transfection (Fig. 1). Moreover, RT-PCR shows a more pronounced reduction of RyR_2 mRNA level compared to protein expression by western blot. This finding is likely due to drastic interference and specific degradation of mRNA by siRNA, indicating that our procedure of RNA silencing is effective in neonatal rat cardiomyocytes.

It is known that $[Ca^{2+}]_i$ occupies a key role in cardiac e–c coupling. During an action potential (AP), the influx of extracellular Ca^{2+} via L-type Ca^{2+} channels triggers SR Ca^{2+} release, resulting in an increase in $[Ca^{2+}]_i$ and myofilament activation [26]. When SR Ca^{2+} content reaches a critical level, spontaneous SR Ca^{2+} release in the form of Ca^{2+} waves or Ca^{2+} oscillations occurs in cardiac cells [27]. The systolic dysfunction observed after transient Ca^{2+} overload is the result of both decreased systolic Ca^{2+} and reduced myofilament sensitivity to Ca^{2+} [28].

In our experiments, we tested the spontaneous Ca^{2+} oscillations and $[Ca^{2+}]_i$ in control and RyR_2 KD cardiomyocytes with aconitine-stimulation (Fig. 3). We found that aconitine induced a sharp increase in the relative $[Ca^{2+}]_i$ and aberrant spontaneous Ca^{2+} oscillations in control cardiomyocytes indicating that the malfunctions of spontaneous Ca^{2+} oscillations and the ability to contract and relax in aconitine-induced cardiomyocytes are due to Ca^{2+} overload of the cytosolic Ca^{2+} concentration. In RyR_2 KD cardiomyocytes with aconitine-stimulation, the spontaneous Ca^{2+} oscillations were recovered partly, also reflects the properties of RyR_2 in aconitine-induced cardiomyocytes. It has been suggested that the occurrence of Ca^{2+} oscillations in RyR_2 (wild type) cells depends completely on the expression of RyR_2 [27], which is consistent with our results that modulating RyR_2 function has a close relationship with the intracellular Ca^{2+} concentration and spontaneous Ca^{2+} oscillations in cardiomyocytes with aconitine-stimulation.

In order to verify whether the overload of the cytosolic Ca^{2+} concentration and the alteration of spontaneous Ca^{2+} oscillations were triggered by excess enhancement of the SR Ca^{2+} release in aconitine-induced cardiomyocytes, we investigated the level of caffeine-induced Ca^{2+} release in control and RyR_2 KD cardiomyocytes.

RyR_2 regulates SR Ca^{2+} release and thus, the Ca^{2+} content of SR luminal storage. We investigated the SR Ca^{2+} release by caffeine stimulation. Rapid application of caffeine solution induces a $[Ca^{2+}]_i$ transient and contracture in cardiomyocytes, and the amplitude

can be used as an index of SR Ca^{2+} releasable content [29]. Fig. 4 demonstrates that higher level of caffeine-induced Ca^{2+} release was observed in both control and RyR_2 KD cardiomyocytes with aconitine-stimulation. These data suggest that aconitine caused enhancing SR Ca^{2+} release by RyR_2 luminal Ca^{2+} activation and an increase in RyR_2 gene expression due to aconitine results in an increase in SR Ca^{2+} leak and intracellular Ca^{2+} concentration. It has been shown that an increase in RyR_2 activity lowered the amplitude of propagating Ca^{2+} waves, but increased the frequency of propagating Ca^{2+} waves and this increase escalates the propensity for triggered arrhythmia [23,24]. An increased propensity for spontaneous Ca^{2+} oscillations and decreased propagating Ca^{2+} waves under the condition of intracellular Ca^{2+} overload triggered by excess enhancement of the SR Ca^{2+} release may underlie a mechanism of aconitine-induced cardiac arrhythmia. It has now become clear that alterations in RyR_2 channel function as a result of genetic defects can cause ventricular arrhythmias [30]. Our findings also provide evidence that acquired dysfunction of RyR_2 could lead to arrhythmia susceptibility.

On the other hand, recent investigations show that SR Ca^{2+} release appears to modulate the sarcolemmal L-type Ca^{2+} currents, suggesting a retrograde communication from the SR to the sarcolemmal L-type Ca^{2+} channels in cardiac e–c coupling [31]. In this regard, it is worthy to identify the effect of aconitine on L-type Ca^{2+} currents in control and RyR_2 KD cardiomyocytes.

As reported, aconitine binds to Na^+ channels and prolongs the voltage-dependent Na^+ channel open state, favoring entry of a large quantity of Na^+ into cytosol. This influx then induces AP and activates the L-type Ca^{2+} currents [32]. In the present study, tetrodotoxin (TTX, 1 μM) was used to inhibit the effect of the Na^+ channel activation induced by aconitine.

As shown in Fig. 5, compared with the control cardiomyocytes, the L-type Ca^{2+} currents were increased in RyR_2 KD cardiomyocytes. Moreover, application of aconitine resulted in a decrease in magnitude of the L-type Ca^{2+} currents in control and RyR_2 KD cardiomyocytes. The physiological function of the L-type current in skeletal muscle fibers is unclear. Some proposal reported that a depletion of SR Ca^{2+} would result in decreased SR Ca^{2+} release on plasma membrane depolarization, resulting in a smaller rise in triadic Ca^{2+}, which in turn would stimulate Ca^{2+} influx via the L-type Ca^{2+} channel [31]. Our results are consistent with the proposal that aconitine stimulation-induced SR Ca^{2+} leakage through RyR_2 channel, which depressed L-type Ca^{2+} current. Our results support the hypothesis of a retrograde communication between the SR Ca^{2+} release channel and the L-type Ca^{2+} channel (DHPR). This communication may be mediated in some cases by a direct interaction between the two channel proteins, L-type Ca^{2+} channel and RyR_2 [33].

Acknowledgments

The authors want to thank Ms. Carlyn Tan from Northwestern University (Chicago) for her help in revising this manuscript. The present work was supported by grants of the ‘Tenth-five’ National Key Technologies R&D Programme (No. 2004BA721A11) and the Ph.D. Programs Foundation of Ministry of Education of China (No. 20060003036).

Abbreviations

RyR_2	type 2-ryanodine receptor
KD	knockdown
e–c coupling	excitation–contraction coupling
ACO	aconitine
SR	sarcoplasmic reticulum
siRNA	small interfering RNA

References

1. Sato H, Yamada C, Konno C, Ohizumi Y, Endo K, Hikino H. Pharmacological actions of aconitine alkaloids. Tohoku J Exp Med. 1979; 128:175–87. [PubMed: 462476]
2. Honerjager P, Meissner A. The positive inotropic effect of aconitine. Naunyn Schmiedebergs Arch Pharmacol. 1983; 322:49–58. [PubMed: 6302523]
3. Hikino H, Konno C, Takata H, Yamada Y, Yamada C, Ohizumi Y. Anti-inflammatory principles of aconitum roots. J Pharm Dyn. 1980; 3:514–25.
4. Herzog W, Feibel R, Bryant S. The effect of aconitine on the giant axon of the squid. J Gen Physiol. 1964; 47:719–33. [PubMed: 14127608]
5. Ameri A. The effects of Aconitum alkaloids on the central nervous system. Prog Neurobiol. 1998; 56:211–35. [PubMed: 9760702]
6. Levy S, Breithardt G, Campbell RW, Camm AJ, Daubert JC, Allessie M, et al. Working Group on Arrhythmias of the European Society of Cardiology. Atrial fibrillation: current knowledge and recommendations for management. Eur Heart J. 1998; 19:1294–320. [PubMed: 9792255]
7. Fu M, Wu M, Wang JF, Qiao YJ, Wang Z. Disruption of the intracellular Ca^{2+} homeostasis in the cardiac excitation-contraction coupling is a crucial mechanism of arrhythmic toxicity in aconitine-induced cardiomyocytes. Biochem Biophys Res Commun. 2007; 354:929–36. [PubMed: 17276394]
8. Eisner DA, Choi HS, Diaz ME, O'Neill SC, Trafford AW. Integrative analysis of calcium cycling in cardiac muscle. Circ Res. 2000; 87:1087–94. [PubMed: 11110764]
9. Bers DM. Cardiac excitation-contraction coupling. Nature. 2002; 415:198–205. [PubMed: 11805843]
10. MacLennan DH, Kranias EG. Phospholamban: a crucial regulator of cardiac contractility. Nat Rev Mol Cell Biol. 2003; 4:566–77. [PubMed: 12838339]
11. Fabiato A. Simulated calcium current can both cause calcium loading in and trigger calcium release from the sarcoplasmic reticulum of a skinned canine cardiac Purkinje cell. J Gen Physiol. 1985; 85:291–320. [PubMed: 2580044]
12. Mickelson JR, Louis CF. Malignant hyperthermia: excitation-contraction coupling, Ca^{2+} release channel, and cell Ca^{2+} regulation defects. Physiol Rev. 1996; 76:537–92. [PubMed: 8618963]
13. Loke J, MacLennan DH. Malignant hyperthermia and central core disease: disorders of Ca^{2+} release channels. Am J Med. 1998; 104:470–86. [PubMed: 9626031]
14. Marx SO, Reiken S, Hisamatsu Y, Jayaraman T, Burkhoff D, Rosemblit N, et al. PKA phosphorylation dissociates FKBP12. 6 from the calcium release channel (ryanodine receptor): defective regulation in failing hearts. Cell. 2000; 101:365–76. [PubMed: 10830164]
15. George CH, Higgs GV, Lai FA. Ryanodine receptor mutations associated with stress-induced ventricular tachycardia mediate increased calcium release in stimulated cardiomyocytes. Circ Res. 2003; 93:531–40. [PubMed: 12919952]
16. Yang HT, Tweedie D, Wang S, Guia A, Vinogradova T, Bogdanov K, et al. The ryanodine receptor modulates the spontaneous beating rate of cardiomyocytes during development. Proc Natl Acad Sci USA. 2002; 99:9225–30. [PubMed: 12089338]

17. Zahabi A, Deschepper CF. Long-chain fatty acids modify hypertrophic responses of cultured primary neonatal cardiomyocytes. J Lipid Res. 2001; 42:1325–30. [PubMed: 11483635]
18. Temsah RM, Netticadan T, Chapman D, Takeda S, Mochizuki S, Dhalla NS. Alterations in sarcoplasmic reticulum function and gene expression in ischemic-reperfused rat heart. Am J Physiol. 1999; 277:H584–94. [PubMed: 10444483]
19. Zhou C, Wen ZX, Shi DM, Xie ZP. Muscarinic acetylcholine receptors involved in the regulation of neural stem cell proliferation and differentiation in vitro. Cell Biol Int. 2004; 28:63–7. [PubMed: 14759770]
20. Knollmann BC, Chopra N, Hlaing T, Akin B, Yang T, Ettensohn K, et al. Casq2 deletion causes sarcoplasmic reticulum volume increase, premature Ca^{2+} release, and catecholaminergic polymorphic ventricular tachycardia. J Clin Invest. 2006; 116:2510–20. [PubMed: 16932808]
21. Reppel M, Sasse P, Piekorz R, Tang M, Roell W, Duan YQ, et al. S100A1 enhances the L-type Ca^{2+} current in embryonic mouse and neonatal rat ventricular cardiomyocytes. J Biol Chem. 2005; 280:36019–28. [PubMed: 16129693]
22. Bassani RA, Bassani JW, Bers DM. Mitochondrial and sarcolemmal Ca^{2+} transport reduce $[Ca^{2+}]_i$ during caffeine contractures in rabbit cardiac myocytes. J Physiol. 1992; 453:591–608. [PubMed: 1464847]
23. Jiang D, Xiao B, Zhang L, Chen SR. Enhanced basal activity of a cardiac Ca^{2+} release channel (ryanodine receptor) mutant associated with ventricular tachycardia and sudden death. Circ Res. 2002; 91:218–25. [PubMed: 12169647]
24. Tiso N, Stephan DA, Nava A, Bagattin A, Devaney JM, Stanchi F, et al. Identification of mutations in the cardiac ryanodine receptor gene in families affected with arrhythmogenic right ventricular cardiomyopathy type 2 ($ARVD_2$). Hum Mol Genet. 2001; 10:189–94. [PubMed: 11159936]
25. Priori SG, Napolitano C, Tiso N, Memmi M, Vignati G, Bloise R, et al. Mutations in the cardiac ryanodine receptor gene ($hRyR_2$) underlie catecholaminergic polymorphic ventricular tachycardia. Circulation. 2001; 103:196–200. [PubMed: 11208676]
26. Seth M, Sumbilla C, Mullen SP, Lewis D, Klein MG, Hussain A, et al. Sarco(endo)plasmic reticulum Ca^{2+} ATPase (SERCA) gene silencing and remodeling of the Ca^{2+} signal mechanism in cardiac myocytes. Proc Natl Acad Sci USA. 2004; 101:16683–8. [PubMed: 15546997]
27. Jiang D, Xiao B, Yang D, Wang R, Choi P, Zhang L, et al. RyR_2 mutations linked to ventricular tachycardia and sudden death reduce the threshold for store-overload-induced Ca^{2+} release (SOICR). Proc Natl Acad Sci USA. 2004; 101:13062–7. [PubMed: 15322274]
28. Holt E, Christensen G. Transient Ca^{2+} overload alters Ca^{2+} handling in rat cardiomyocytes: effects on shortening and relaxation. Am J Physiol. 1997; 273:H573–82. [PubMed: 9277471]
29. Catterall WA, Trainer V, Baden DG. Molecular properties of the sodium channel: a receptor for multiple neurotoxins. Bull Soc Pathol Exot. 1992; 85:481–5. [PubMed: 1340350]
30. Zhang XQ, Song J, Rothblum L, Lun M, Wang X, Ding F, et al. Overexpression of Na^+/Ca^{2+} exchanger alters contractility and SR Ca^{2+} content in adult rat myocytes. Am J Physiol Heart Circ Physiol. 2001; 281:H2079–88. [PubMed: 11668069]
31. Balog EM, Gallant EM. Modulation of the sarcolemmal L-type current by alteration in SR Ca^{2+} release. Am J Physiol. 1999; 276:C128–35. [PubMed: 9886928]
32. Sterling NW. Comparison of aconitine-modified human heart (hH1) and rat skeletal (μ1) muscle Na^+ channels: an important role for external Na^+ ions. J Physiol. 2002; 538:759–71. [PubMed: 11826163]
33. Nakai J, Dirksen RT, Nguyen HT, Pessah IH, Beam KG, Allen PD. Enhanced dihydropyridine receptor channel activity in the presence of ryanodine receptor. Nature. 1996; 6380:72–5. [PubMed: 8598910]

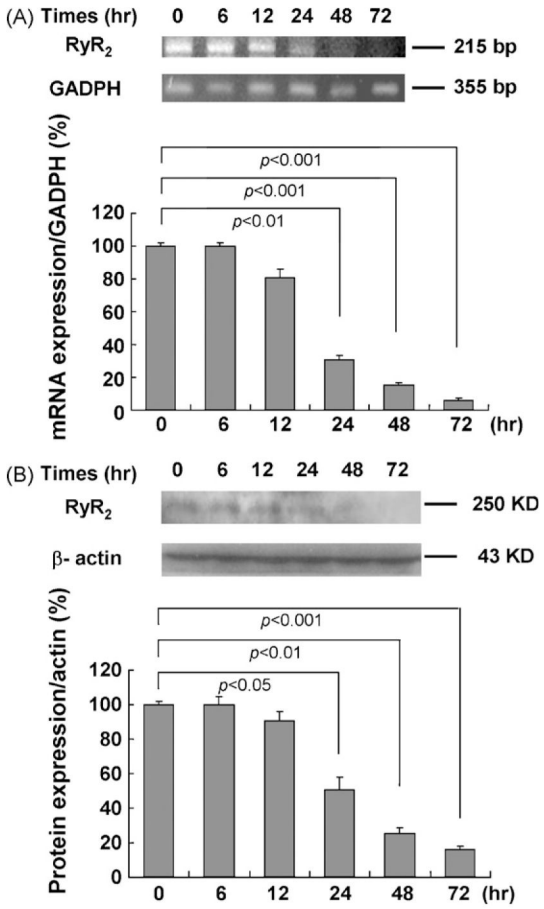

Fig. 1.

Effects of siRNA3 target on mRNA and protein levels of RyR_2 in rat primary cardiomyocytes with transfection after 6–72 h tested by RT-PCR and western blot. (A) Changes in mRNA levels of RyR_2 in cardiomyocytes with siRNA3 transfection after 6–72 h. GAPDH served as an internal control for analysis of the PCR productions. (B) Changes in protein expressions of RyR_2 in cardiomyocytes with siRNA3 transfection after 6–72 h. β-Actin was used as a standard for analysis of the protein samples. Data are presented as the mean ± S.E. Differences were considered statistically significant when p-value <0.05, t-test, $n = 4$.

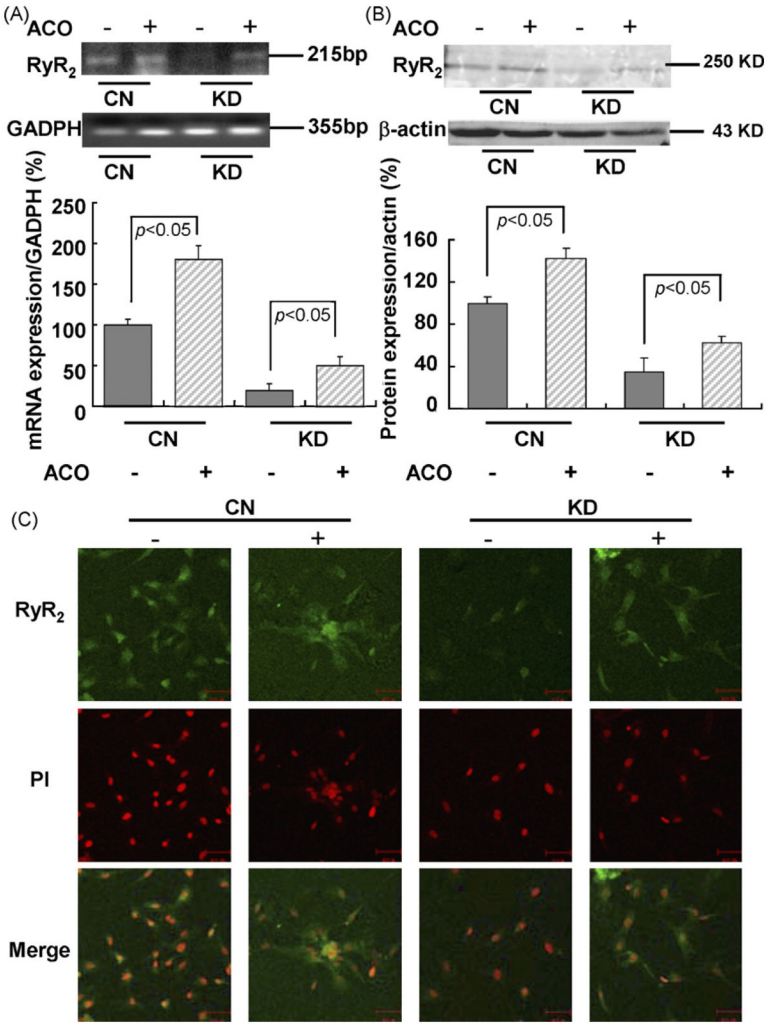

Fig. 2.

Effects of aconitine on mRNA and protein levels of RyR_2 in control cardiomyocytes and knockdown cardiomyocytes (with siRNA3 transfection after 48 h) tested by RT-PCR, western blot, and immunostaining. (A and B) Changes in mRNA and protein levels of RyR_2 in CN and KD cardiomyocytes before and after aconitine application for 0.5 h. GAPDH and β-actin were used as standards for analyses of the protein and total RNA samples, respectively. Data are presented as the mean ± S.E. Differences were considered statistically significant when p-value <0.05, t-test, $n = 4$. (C) Immunostaining of RyR_2 fluorescence in CN and KD cardiomyocytes before and after aconitine application, respectively, using the anti-RyR primary antibody (scale bar: 50 μm). Immunofluorescence staining on cardiomyocytes RyR positive signals is better observed in the cytosol (green signals). All nuclei were stained with PI (CN, control; KD, knockdown; ACO, aconitine).

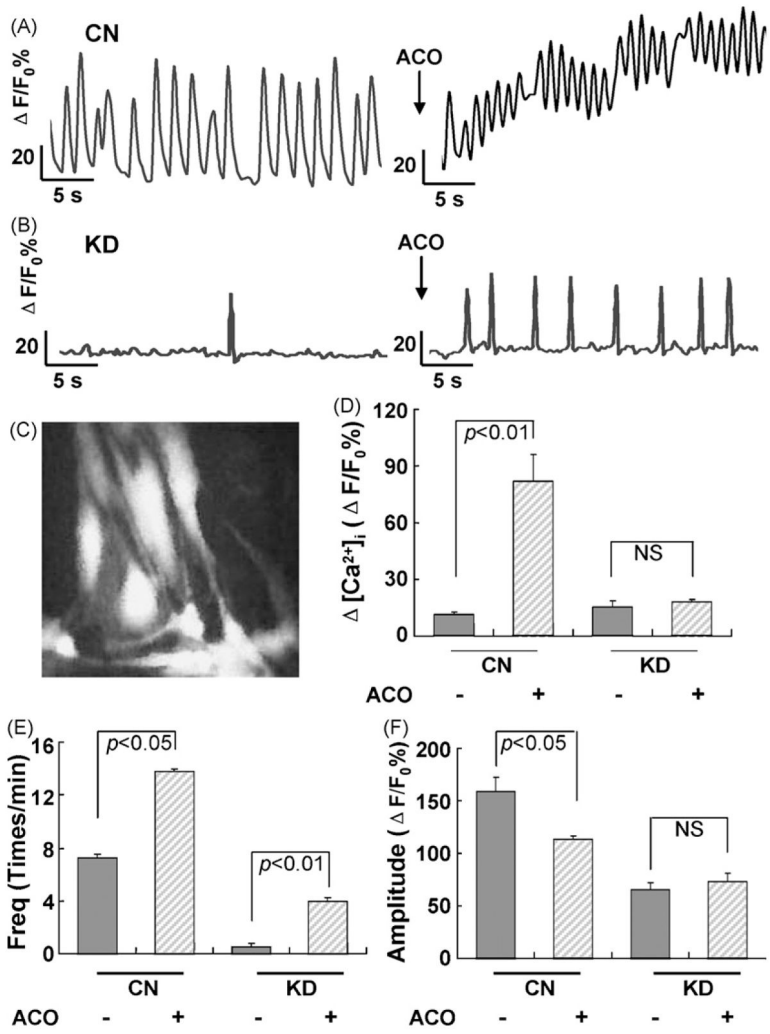

Fig. 3.

Effects of aconitine on the relative intracellular Ca^{2+} concentration and spontaneous Ca^{2+} oscillations in control cardiomyocytes and knockdown cardiomyocytes (with siRNA3 transfection after 48 h) examined by Ca^{2+} imaging. (A and B) Representative recordings of the spontaneous Ca^{2+} oscillations in a given CN and KD cardiomyocyte before and after aconitine application, respectively. Traces indicate relative changes of fluo-3 intensity ($\Delta F/F_0$%) over time in cells randomly selected from the culture dish. Each trace represents $\Delta F/F_0$% of an individual cell acquired every 5 s. (C) The photograph shows fluorescent image of cardiomyocytes loaded with fluo-3 AM (scale bar: 50 μm). (D–F) Effects of aconitine on the baseline $[Ca^{2+}]_i$, the frequency and amplitude of spontaneous Ca^{2+} oscillations in CN and KD cardiomyocyes before and after aconitine application. Data are presented as the mean ± S.E. Differences were considered statistically significant when *p*-value <0.05, *t*-test, $n = 4$ plates (CN, control; KD, knockdown; ACO, aconitine).

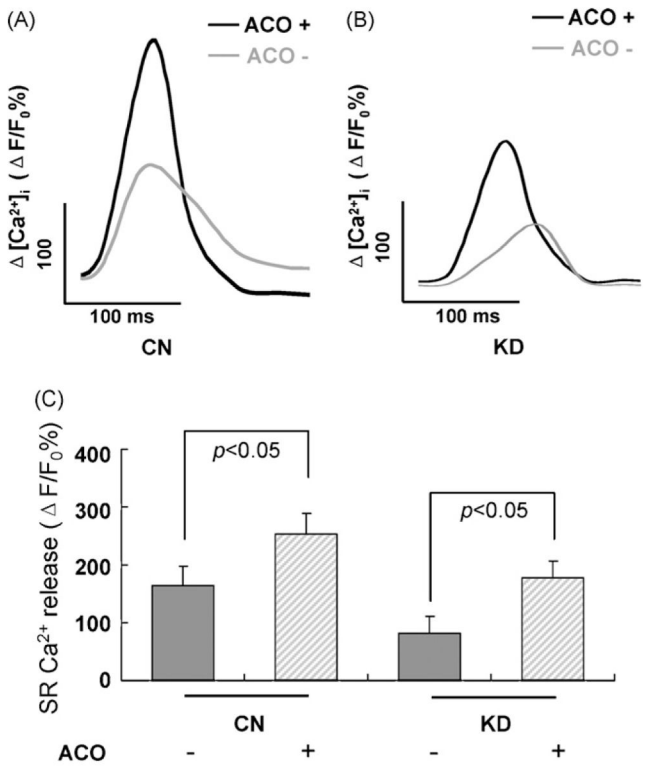

Fig. 4.

Effects of aconitine on sensitivity to caffeine contracture in control cardiomyocytes and knockdown cardiomyocytes (with siRNA3 transfection after 48 h) examined by Ca^{2+} imaging. (A and B) Caffeine-induced Ca^{2+} transients in CN and KD cardiomyocytes before (gray trace) and after (black trace) aconitine application for 5 min. Each trace represents $\Delta F/F_0$% of an individual cell acquired every 200 ms. (C) Average $\Delta[Ca^{2+}]_i$ for caffeine-induced Ca^{2+} transients. Data are presented as the mean ± S.E. Differences were considered statistically significant when *p*-value <0.05, *t*-test, $n = 5$ cells per plate, four plates (CN, control; KD, knockdown; ACO, aconitine).

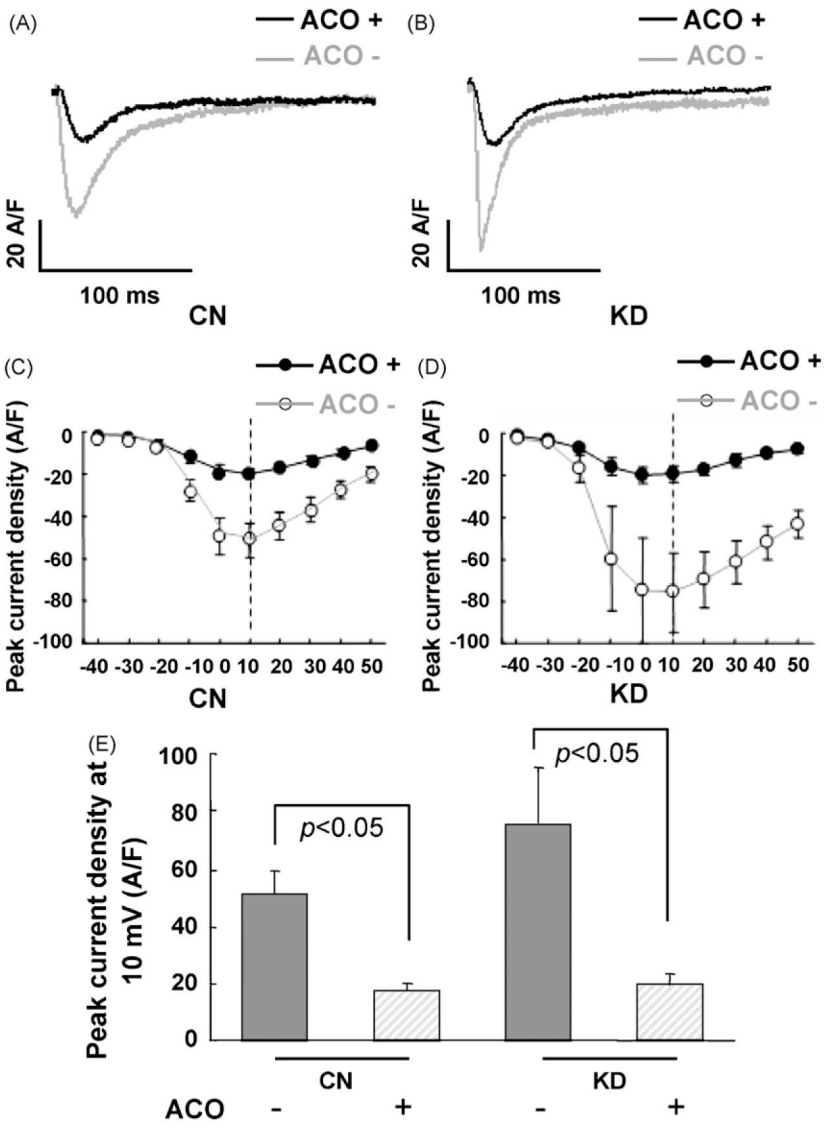

Fig. 5.

Effects of aconitine on the L-type Ca^{2+} currents in control cardiomyocytes and knockdown cardiomyocytes (with siRNA3 transfection after 48 h) examined by patch clamp. (A and B) L-type Ca^{2+} currents recorded at 10 mV command potential in CN and KD cardiomyocyes before (gray trace) and after (black trace) aconitine application for 5 min. (C and D) I_{Ca}–V relationships in CN (hollow circle) and KD cardiomyocytes (solid circle) before (gray trace) and after (black trace) aconitine application. (E) Peak current density at 10 mV command potential in CN and KD cardiomyocyes. Data are presented as the mean ± S.E. Differences were considered statistically significant when p-value <0.05, t-test, n = 5 cells per plate, five plates (CN, control; KD, knockdown; ACO, aconitine).